

MEOP CONTROL DESIGN SYNTHESIS:
OPTIMAL QUANTIFICATION OF THE MAJOR DESIGN TRADEOFFS

D. C. Hyland
and
D. S. Bernstein
Harris Corporation
Government Aerospace Systems Division
Melbourne, Florida

Workshop on Structural Dynamics and Control Interaction
of Flexible Structures
MSFC, Huntsville, Alabama
April 22-24, 1986

INTRODUCTION: OPTIMAL PROJECTION/MAXIMUM ENTROPY DESIGN SYNTHESIS

In this presentation we (1) discuss the underlying philosophy and motivation of the optimal projection/maximum entropy (OP/ME) stochastic modelling and reduced order control design methodology for high order systems with parameter uncertainties, (2) review the OP/ME design equations for reduced-order dynamic compensation including the effect of parameter uncertainties, and (3) illustrate the application of the methodology to several Large Space Structure (LSS) problems of representative complexity. The basis for this paper is references [1-25] along with recently obtained results.

The OP/ME approach, as its name suggests, represents the synthesis of two distinct ideas: (1) reduced-order dynamic compensator design for a given high-order plant (i.e., optimal projection design) and (2) minimum-information stochastic modelling of parameter uncertainties (i.e., maximum entropy modelling). Maximum entropy modelling is discussed in [1-13,15] and optimal projection design is studied in [6,10,12,14,16-25].

Before attempting an overview of the OP/ME approach, it is important to discuss the class of problems that motivated this work, namely, control of large flexible space structures. A finite-element model of a large flexible space structure is, generally, an extremely high-order system. For example, a version of the widely studied CSDL Model #2 includes 150 modes and 6 disturbance states, i.e., a total of 306 states, along with 9 sensors and 9 actuators. The size of the model and the coupling between sensors and actuators render classical control-design methods useless and all but confound attempts to use LQG to obtain a controller of manageable order. Indeed, these difficulties were a prime motivation for the optimal projection approach. Besides the high order of these systems, finite element modelling is known to have poor accuracy, particularly for the high-order modes. Reasonable and not overly conservative uncertainty estimates predict 30-50 percent error in modal frequencies after the first 10 modes, with the situation considerably more complex (and pessimistic) for damping estimates. Otherwise-successful control-design methodologies widely promulgated in the aerospace community were severely strained in the face of such difficulties.

As indicated in Figure 1, maximum entropy modelling addresses the robustness problem by permitting direct inclusion of parameter uncertainties in the plant and disturbance models so that quadratically optimal system design plus maximum entropy modelling automatically yield system designs that trade performance off against modelling uncertainties. Furthermore, complexity and cost generally preclude implementation of very high dimension controllers (as in standard LQG techniques). Optimal projection design deals directly and rigorously with the question of system dimension by trading controller order off against performance.

OPTIMAL PROJECTION/MAXIMUM ENTROPY DESIGN SYNTHESIS

- **Parameter uncertainties are directly incorporated into the design process**
 - ⇒ **Optimal quantification of robustness/performance tradeoff**
- **Controller order fixed by implementation constraints**
 - ⇒ **Optimal quantification of order/performance tradeoff**

Figure 1

MAXIMUM ENTROPY MODELLING

Maximum entropy modelling is a form of stochastic modelling. Although external disturbances are traditionally modelled stochastically as random processes, the use of stochastic theory to model plant parameter uncertainty has seen relatively limited application. All objections to a stochastic parameter uncertainty model are dispelled by invoking the modern information-theoretic interpretation of probability theory. Rather than regarding the probability of an event as the limiting frequency of numerous repetitions (as, e.g., the number of heads in 1,000 coin tosses) we adopt the view that the probability of an event is a quantity which reflects the observer's certainty as to whether a particular event will or will not occur. This quantity is nothing more than a measure of the information (including, e.g., all theoretical analysis and empirical data) available to the observer. In this sense the validity of a stochastic model of a flexible space structure, for example, does not rely upon the existence of a fleet of such objects (substitute "ensemble" for "fleet" in the classical terminology) but rather resides in the interpretation that it expresses the engineer's certainty or uncertainty regarding the values of physical parameters such as stiffnesss of structural components. This view of probability theory has its roots in Shannon's information theory but was first articulated unambiguously by Jaynes (see [26-29]).

The preeminent problem in modelling the real world is thus the following: given limited (incomplete) a priori data, how can a well-defined (complete) probability model be constructed which is consistent with the available data but which avoids inventing data which does not exist? To this end we invoke Jaynes' Maximum Entropy Principle: First, define a measure of ignorance in terms of the information-theoretic entropy, and then determine the probability distribution which maximizes this measure subject to agreement with the available data. The smallest collection of data for which a well-defined probability model (called the minimum information model) can be constructed is known as the minimum data set.

The reasoning behind this principle is that the probability distribution which maximizes a priori ignorance must be the least presumptive (i.e., least likely to invent data) on the average since the amount of a posteriori learned information (should all uncertainty suddenly disappear) would necessarily be maximized. If, for some probability distribution, the a priori ignorance and hence the a posteriori learning were less than their maximum value then this distribution must be based upon invented and, hence, generally incorrect data. The Maximum Entropy Principle is clearly desirable for control-system design where the introduction of false data is to be assiduously avoided.

It is shown in [1] that the stochastic model induced by the Maximum Entropy Principle of Jaynes is a Stratonovich multiplicative white noise model. The earlier developments considered a relatively restricted class of parameter uncertainties. At present, however, the theory extends to the most general modelling uncertainties encountered in flexible mechanical systems. Moreover, the minimum data set presently used to induce the maximum entropy stochastic model consists of stipulated bounds on the deviations of physical parameters about their nominal values. This description is both convenient and deeply rooted in engineering tradition. As indicated in Figure 2, these parameter bounds are the basic data needed to implement maximum entropy modelling in practice.

MINIMUM-INFORMATION MODELLING

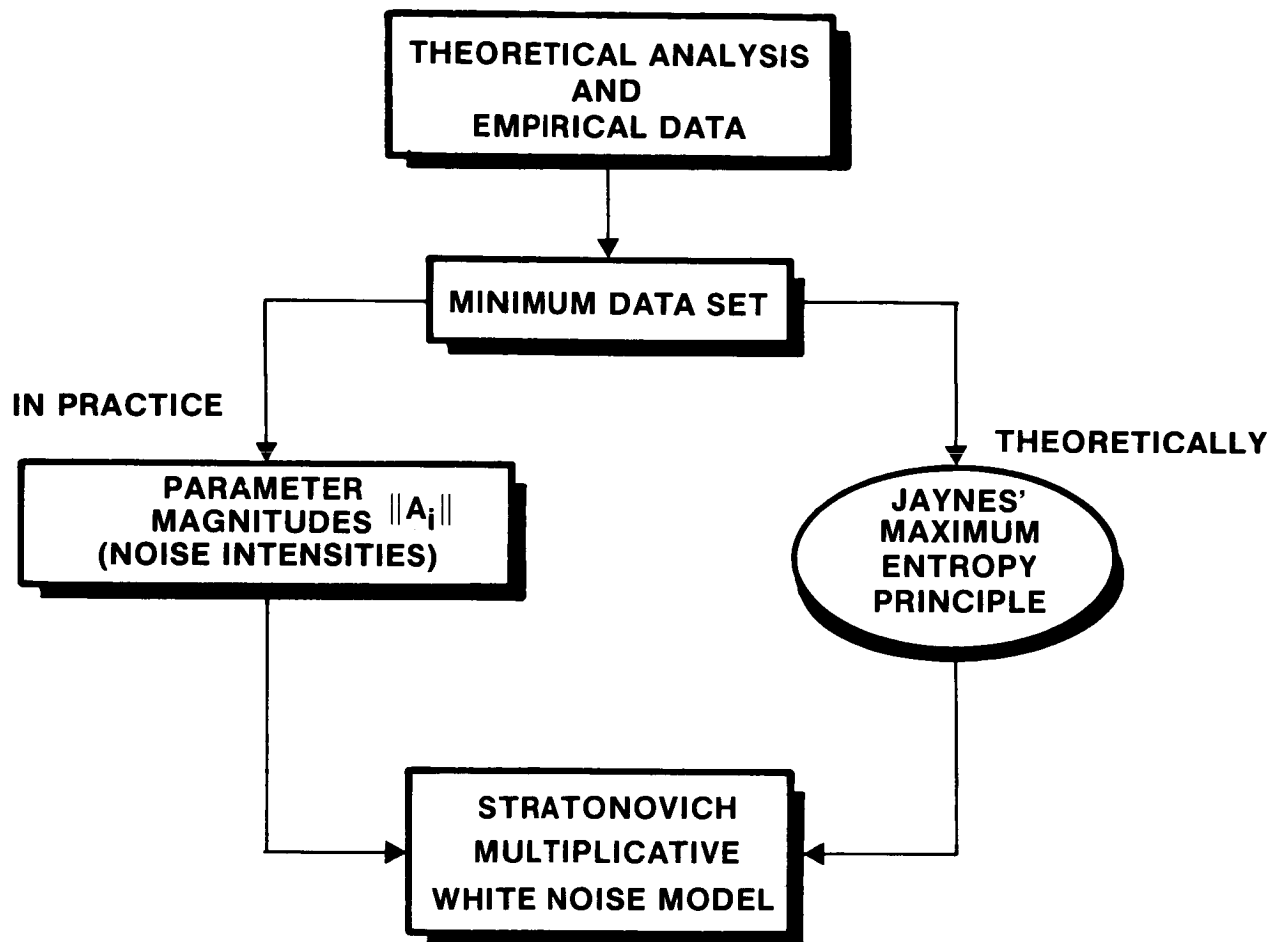


Figure 2

REPRESENTATION OF PARAMETER UNCERTAINTIES

Once significant types of parameter uncertainty have been identified and bounds on parameter variations established, the maximum entropy model can be placed in the general form shown in Figure 3. The set $\{A_i, i=1, \dots, N\}$ of deterministic matrices defines the geometric pattern of the uncertain perturbation, ΔA , of the dynamics matrix. The norm $\|A_i\|$ defines the magnitude of uncertainty and is uniquely related to the originally stipulated parameter deviation bound. The stochastic model which follows in consequence of Jayne's Maximum Entropy Principle is a form of Stratonovich white noise. This model is extremely mathematically tractable since the second moment equation for the state can be closed. Moreover, the Stratonovich formulation allows crucial effects of uncertainty to be reproduced.

A = Nominal Dynamics Matrix

A + ΔA = Actual Dynamics Matrix (But ΔA Is Unknown)

WHITE NOISE REPRESENTATION

$$\Delta A = \sum_{i=1}^p \alpha_i(t) A_i$$

$\alpha_i(t)$ = Zero-Mean, Unit-Intensity, Uncorrelated White Noise Processes

A_i = Uncertainty Pattern

$\|A_i\|$ = Uncertainty Magnitude

MULTIPLICATIVE WHITE NOISE MODEL

$$\dot{x}(t) = (A + \sum_{i=1}^p \alpha_i(t) A_i) x(t)$$

Figure 3

STOCHASTIC DIFFERENTIAL EQUATIONS AND THE STRATONOVICH CORRECTION

Figure 4 displays the stochastic differential equation (second equation in the figure) arising from the Stratonovich model. To illustrate the crucial features of this model, a brief review of the literature on multiplicative white noise is absolutely essential. The theory of stochastic differential equations was placed on a firm mathematical foundation by Ito [30] and has been widely developed and applied to modelling, estimation and control problems [31-59]. The basic linear multiplicative white noise model is given by the Ito differential equation:

$$dx_t = (A dt + \sum_{i=1}^p d\alpha_{it} A_i) X_t$$

where the $d\alpha_{it}$ are Wiener processes. Although such models were studied extensively for estimator and control design [40-56], this approach fell into disrepute with the publication of [58,59] where it was shown for discrete-time systems that sufficiently high uncertainty levels (i.e., magnitudes $\|A_i\|$ above a threshold) led to the nonexistence of a steady state solution. Although it was purported in [58] that this "phenomenon" was an "obvious" consequence of high uncertainty levels, these conclusions failed to take into account (possibly because of the discrete-time setting) the subtle relationship between the ordinary differential equation (the first equation in Figure 4) and the stochastic differential equation. Indeed, it was shown in [31] that if a stochastic differential equation is regarded as the limit of a sequence of ordinary differential equations, then the above Ito equation is not correct. Instead, the ordinary differential equation with multiplicative white noise corresponds to the corrected Ito equation appearing as the second equation in Figure 4. It is seen that this differs from the "naive" equation by a systematic drift term (the Stratonovich correction). Although skepticism regarding this unusual result was admitted to in [31], the form of the second equation in Figure 4 was corroborated completely independently by Stratonovich in [32], whose results actually appeared in the Russian literature prior to 1965. His approach is based upon an alternative definition of stochastic integration which differs from Ito stochastic integration by a mathematical technicality. The Stratonovich approach, it should be noted, has the interesting feature that approximating sums involve future values of a Brownian motion process which, although physically unacceptable in the classical view of probability, is completely consistent with the information-theoretic interpretation.

In spite of the glaring technicality of the Stratonovich correction, almost all research on the estimation and control of such systems failed to perceive its physical significance. To the author's knowledge, the work of Gustafson and Speyer [56] was the only paper prior to the appearance of [1] which demonstrated the crucial feature: The Stratonovich correction neutralizes the threshold uncertainty principle. In particular for systems which are inherently stable under particular parameter variations (e.g., structures with uncertain stiffness matrices), the Stratonovich formulation correctly predicts unconditional second-moment stability - in contrast to the Ito formulation within which a stringent uncertainty threshold is encountered.

STRATONOVICH CORRECTION

Stratonovich, 1966 [31]; Wong and Zakai, 1965 [32]

Ordinary Differential Equation: $\dot{x}(t) = (A + \sum_{i=1}^p \alpha_i(t) A_i) x(t)$

Itô Stochastic Differential Equation: $dx_t = (A_s dt + \sum_{i=1}^p d\alpha_{it} A_i) x_t$

$$A_s = A + \underbrace{\frac{1}{2} \sum_{i=1}^p A_i^2}_{\text{correction}}$$

Figure 4

MAXIMUM ENTROPY MODIFICATION OF THE STATE COVARIANCE EQUATION

Note that when undertaking quadratic optimization within the maximum entropy model, one minimizes the mathematical expectation of the usual quadratic performance penalty taken over the maximum entropy statistics. Thus the feature of the stochastic model most utilized in practice is the second moment equation for the system state. The form of this equation that results from the Stratonovich white noise model is given explicitly in Figure 5. The "stochastic modification" term given by the bottom expression in Figure 5 distinguishes this stochastic Lyapunov equation from the ordinary Lyapunov equation that would result from a deterministically parametered model.

The importance of the stochastic modification term cannot be underrated. In particular, for most types of parameter uncertainty encountered in structural systems, the Stratonovich corrections in $M[Q]$ imply progressive decorrelation between pairs of dynamical states. This informational or statistical damping phenomenon is a direct result of parameter uncertainties that is captured by the multiplicative white noise model. The Stratonovich correction, moreover, is crucial: By neutralizing the threshold uncertainty principle, it permits the consideration of long-term effects for arbitrary uncertainty levels.

$$\dot{Q}(t) = A_s Q(t) + Q(t) A_s^T + \sum_{i=1}^p A_i Q(t) A_i^T + V$$

$$Q(t) = E[x(t)x(t)^T] \quad (\text{The quantity of interest in quadratic optimization})$$

E = Average over parameter uncertainties and disturbances

$$A_s = A + \frac{1}{2} \sum_{i=1}^p A_i^2 \qquad V = \text{Disturbance Intensity}$$

STOCHASTIC MODIFICATION

$$M[Q] = \frac{1}{2} \left(\sum_{i=1}^p A_i^2 Q + Q \sum_{i=1}^p A_i^2 T \right) + \sum_{i=1}^p A_i Q A_i^T$$

Figure 5

RAMIFICATIONS FOR THE STRUCTURE OF THE STEADY STATE COVARIANCE

The far-reaching ramifications of the foregoing observations are explored extensively in [1-10]. As an example, assume (as is usually the case in practice) that uncertainties in modal frequency obtained from a finite-element analysis of a large flexible space structure increase with mode number. From the form of $M[Q(t)]$ it is easy to deduce that the steady state covariance becomes increasingly diagonally dominant with increasing frequency and thus assumes the qualitative form given in Figure 6. The benefits of this sparse form are important: The computational effort required to determine the steady state covariance (and thus to design a closed-loop controller, for example) is directly proportional to the amount of information reposed in the model or, equivalently, inversely proportional to the level of modelled parameter uncertainty. This casts new light on the computational design burden vis-a-vis the modelling question: The computational burden depends only upon the information actually available. A simple control-design exercise involving full-state feedback for a simply supported beam presented in [4] illustrates this point. The gains for the higher-order modes of the beam, whose frequency uncertainties increase linearly with frequency, were obtained with modest computational effort in spite of 100 structural modes included in the model. Another important ramification of the qualitative form of Q is the automatic generation of a high/low-authority control law. Note that for the higher order and hence highly uncertain modes the control gains reported in [3,4] indicated an inherently stable, low performance rate-feedback control law, whereas for the lowest order modes the control law is high authority, i.e., "LQ" in character.

EFFECT OF FREQUENCY UNCERTAINTIES ON THE QUALITATIVE STRUCTURE OF THE STEADY-STATE COVARIANCE $Q = \lim_{t \rightarrow \infty} E[x(t)x(t)^T]$

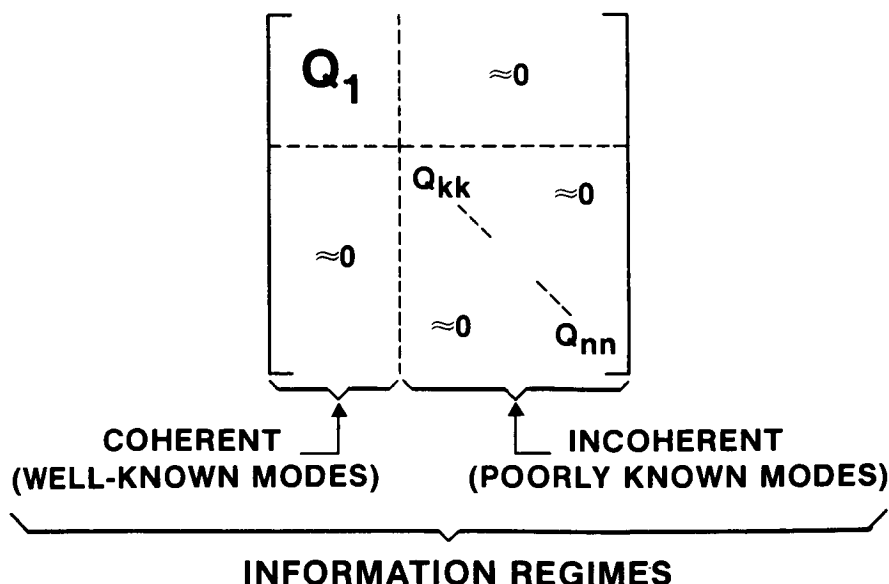


Figure 6

PERFORMANCE ROBUSTNESS

Figure 7 illustrates the basic concept of robustness with respect to performance that is so essential to adequate LSS control design. The curves shown sketch the variation of closed-loop performance (e.g., line-of-sight error) for particular control designs when system parameters deviate from their nominal values. As illustrated in one example below, standard LQG design provides a sharp minimum at the nominal parameter values but can be extremely sensitive to off-nominal variations. On the other hand, since the maximum entropy formulation includes the deleterious effects of uncertainty within the basic design model, it provides the mechanism to assure satisfaction of performance objectives not only for the nominal model but also over the likely range of parameter deviations. Note that the price paid for this is a degradation of performance (relative to a deterministic model, LQG design) whenever the system parameters happen to be near their nominal values. However, this tradeoff between nominal performance and robustness is widely recognized as an inescapable fact of life. The prime motivation for the maximum entropy development is to achieve a design methodology which sacrifices as little near-nominal performance as possible while securing performance insensitivity over the likely range of modelling errors.

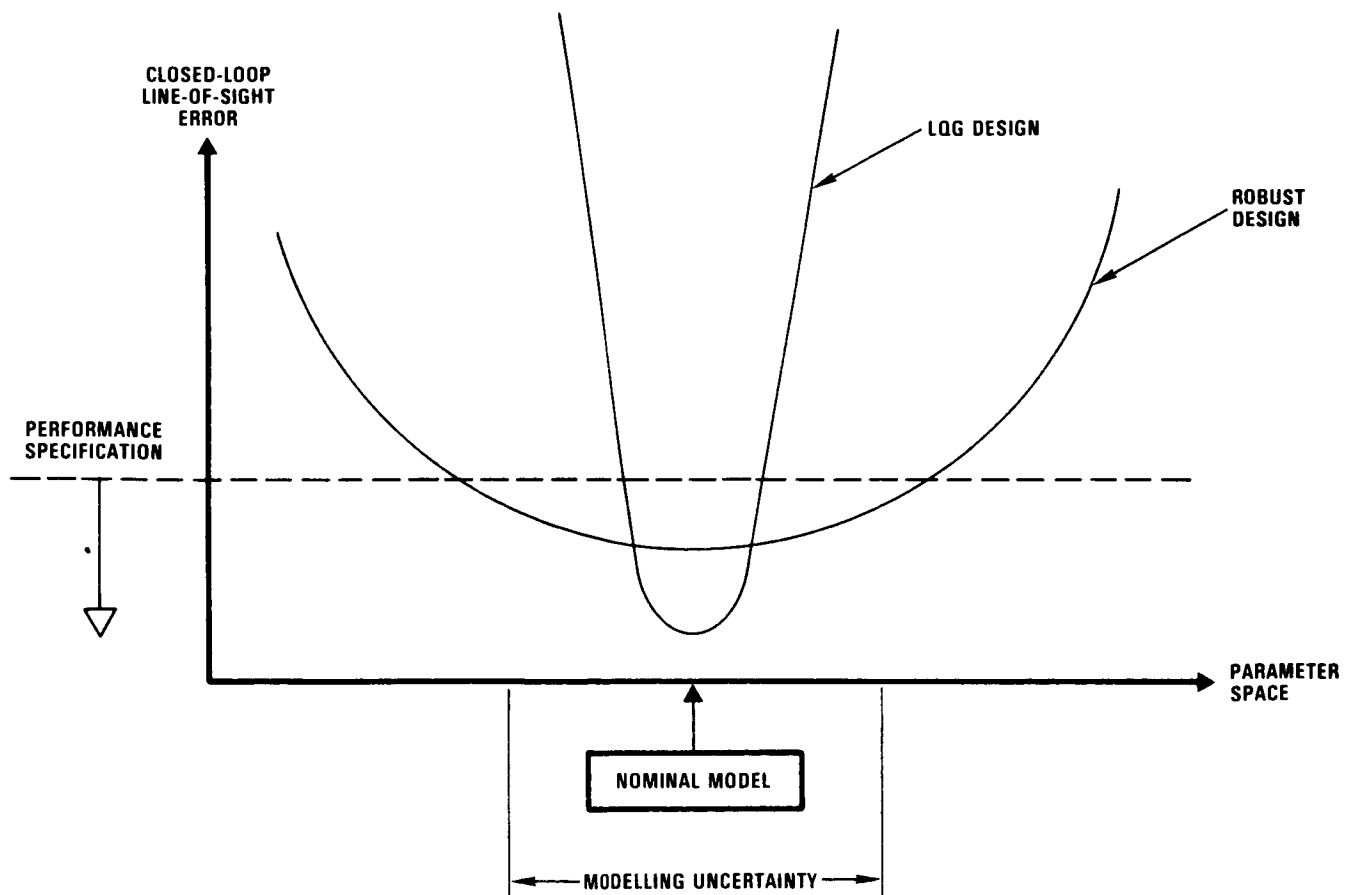


Figure 7

DEVELOPMENT OF THE OP/ME SYNTHESIS

At this point, we consider the optimal projection approach and its amalgamation with maximum entropy modelling. Figure 8 illustrates that the overall development proceeded along two distinct paths, starting from standard LQG theory. One path of development (the right branch) retained the LQG assumption that the dynamic controller to be designed is of the same dimension as the plant but extended the theory by including the effects of parameter uncertainty via stochastic modelling. The optimality conditions for full-order dynamic compensation under a maximum entropy model are the principal design results and consist of two modified Riccati equations coupled to two Lyapunov equations by the stochastic modification terms. These equations were presented in [5,15] and were also independently discovered by a Soviet researcher [57].

The second path of development from LQG retained the assumption of a deterministically parametered model but removed the restriction to full-order compensation - i.e., a quadratically optimal but fixed-order compensator is sought for a higher order plant in order to simplify implementation. This led to the optimal projection approach to fixed-order compensation.

The optimal projection approach is based entirely on a theorem which characterizes the quadratically optimal reduced-order dynamic compensator. Assuming a purely dynamic linear system structure for the desired compensator whose order is determined by implementation constraints (e.g., reliability, complexity or computing capability), a parameter optimization approach is taken. There is, of course, nothing novel about this approach per se and it has been widely studied in the control literature [60-73]. Clearly, the parameter optimization approach fell into disrepute because of the extreme complexity of the grossly unwieldy first-order necessary conditions which afforded little insight and engendered brute force gradient search techniques. The crucial discovery occurred in [6] where it was revealed that the necessary condition for the dynamic-compensation problem gives rise to the definition of an optimal projection as a rigorous, unassailable consequence of quadratic optimality without recourse to ad hoc methods as in [74-83]. Exploitation of this projection leads to immense simplification of the "primitive" form of the necessary conditions for this problem. The novel equations consist of two modified Riccati equations and two modified Lyapunov equations (analogous to the four optimality conditions for full-order compensation under maximum entropy models) coupled, in this instance, by a projection of rank equal to the desired controller dimension. This "optimal projection" essentially characterizes the geometric structure of a reduced-order plant model employed internally by the compensator.

OPTIMAL PROJECTION/MAXIMUM ENTROPY APPROACH TO LOW-ORDER, ROBUST CONTROLLER DESIGN

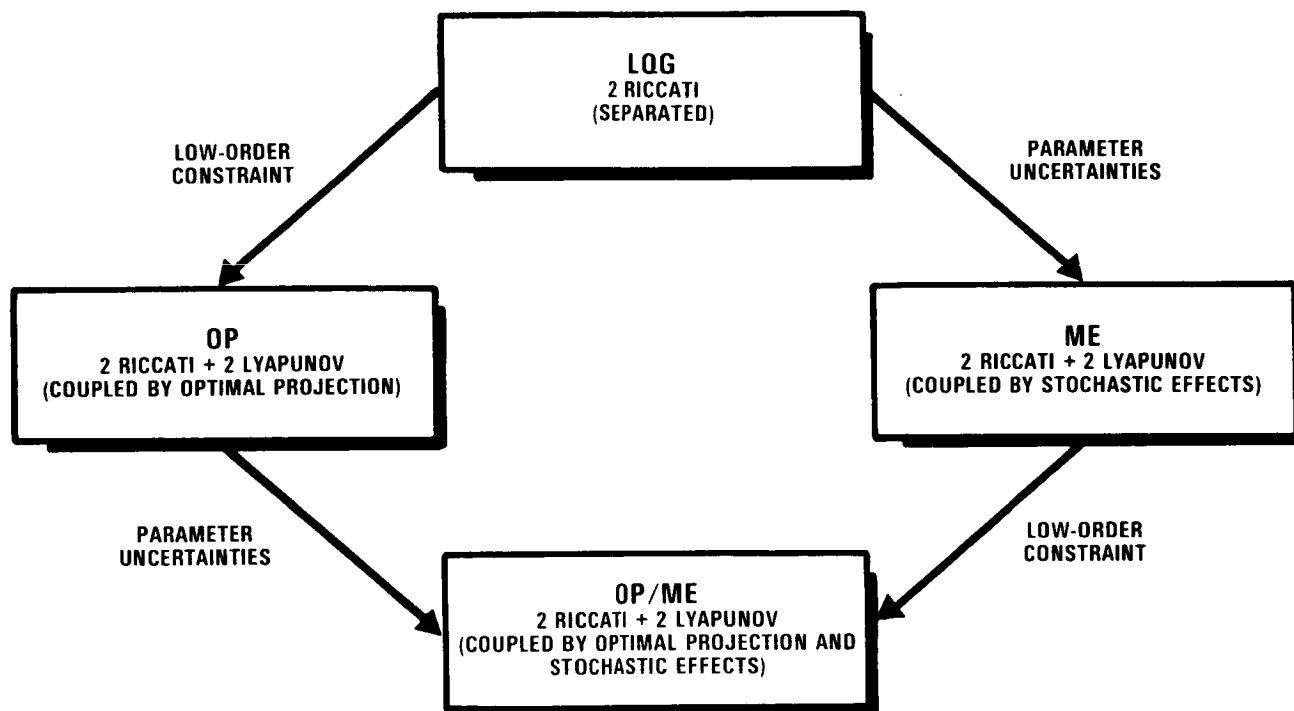


Figure 8

SURVEY OF APPROACHES TO FIXED-ORDER DYNAMIC COMPENSATOR DESIGN

Before describing the synthesis of the optimal projection (OP) and maximum entropy (ME) approaches, we sketch the relationship between optimal projection and previously proposed techniques for reduced-order compensator design. The general relationships among general categories of approaches are illustrated in Figure 9.

The basic premise is that the plant to be controlled is distributed parameter in character (as are structural systems). The usual engineering approach (the right branch in Figure 9) is to replace the distributed parameter system with a high-order finite-dimensional model. However, fundamental difficulties remain since application of LQG leads to a controller whose order is identical to that of the high-order approximate model. Attempts to remedy this problem usually rely upon some method of open-loop model reduction followed by LQG design or LQG design followed by closed-loop controller reduction (see, e.g., [74-83]). Most of these techniques are ad hoc in nature, however, and hence guarantees of optimality and stability are lacking.

A more direct approach that avoids both model and controller reduction is to fix the controller structure and optimize the performance criterion with respect to the controller parameters. This is the optimal projection formulation. As noted above, the new forms of optimality conditions discovered in [6] harbor the definition of an oblique projection (i.e., idempotent matrix) which is a consequence of optimality and not the result of an ad hoc assumption. By exploiting the presence of this "optimal projection," the originally very complex stationary conditions can be transformed without loss of generality into much simpler and more tractable forms. The resulting equations (see (2.10)-(2.17) of [22]) preserve the simple form of LQG relations for the gains in terms of covariance and cost matrices which, in turn, are determined by a coupled system of two modified Riccati equations and two modified Lyapunov equations. This coupling, by means of the optimal projection, represents a graphic portrayal of the demise of the classical separation principle for the reduced-order controller case. When, as a special case, the order of the compensator is required to be equal to the order of the plant, the modified Riccati equations immediately reduce to the standard LQG Riccati equations and the modified Lyapunov equations express the proviso that the compensator be minimal, i.e., controllable and observable. Since the LQG Riccati equations as such are nothing more than the necessary conditions for full-order compensation, the "optimal projection equations" appear to provide a clear and simple generalization of standard LQG theory.

On the other hand (see the left branch of Figure 9), the approach taken by the mathematical community accepts the distributed parameter model, extends LQG results to obtain a controller of similarly infinite dimensional nature and then resorts to discretization and truncation to achieve a suitably low-order (and finite dimensional) controller for implementation. However, the finite-dimensional approximation schemes that have been applied to optimal infinite-dimensional control laws [84-87] only guarantee optimality in the limit, i.e., as the order of the approximating controller increases without bound. Hence, there is no guarantee that a particular approximate (i.e., discretized) controller is actually optimal over the class of approximate controllers of a given order which may be dictated by implementation constraints. Moreover, even if an optimal approximate finite-dimensional controller could be obtained, it would almost certainly be suboptimal in the class of all controllers of the given order.

It should be mentioned that notable exceptions to the above-mentioned work on distributed parameter controllers are the contributions of Johnson [88] and Pearson [89,90] who suggest fixing the order of the finite-dimensional compensator while retaining the distributed parameter model. Progress in this direction, however, was impeded not only by the intractability of the optimality conditions that were available for the finite-dimensional problem, but also by the lack of a suitable generalization of these conditions to the infinite-dimensional case. Recent results [18,21,23] made significant progress in filling these gaps by deriving explicit optimality conditions which directly characterize the optimal finite-dimensional fixed-order dynamic compensator for an infinite-dimensional system and which are exactly analogous to the highly simplified optimal projection equations obtained in [6,12,14,16,22] for the finite-dimensional case. Specifically, instead of a system of four matrix equations we obtain a system of four operator equations whose solutions characterize the optimal finite-dimensional fixed-order dynamic compensator. Moreover, the optimal projection now becomes a bounded idempotent Hilbert-space operator whose rank is precisely equal to the order of the compensator.

As Figure 9 suggests, this represents the most direct approach yet taken to designing low-order controllers for infinite-dimensional systems. Computational techniques for solution of the operator equations remain the object of research, but success in the finite-dimensional case leads to confidence that existing solution techniques can be appropriately generalized.

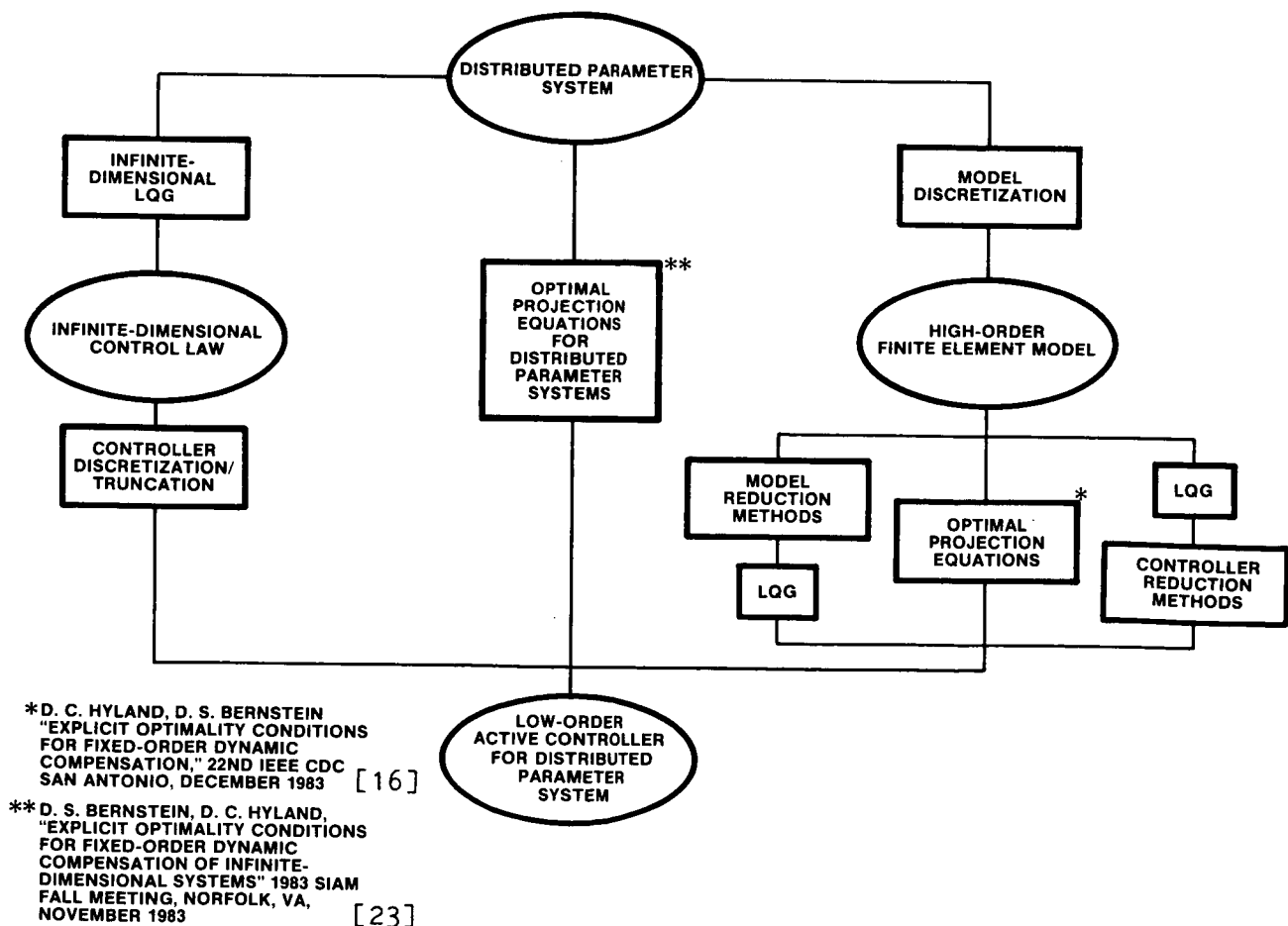
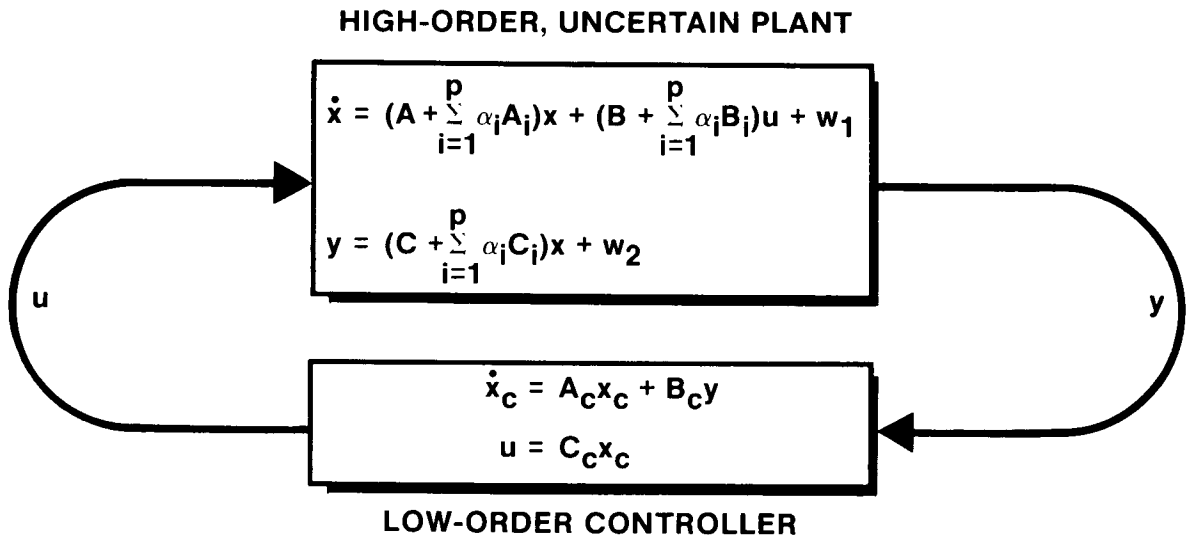


Figure 9

STEADY STATE REDUCED-ORDER DYNAMIC COMPENSATION PROBLEM WITH PARAMETER UNCERTAINTIES

Now we explicitly present the combined OP/ME design equations. First, Figure 10 gives the problem statement. The high-order, uncertain plant has state $x \in \mathbb{R}^N$ where N is finite. As indicated using previous notation, uncertainties in the dynamics matrix, A , the control input matrix, B , and the sensor output matrix, C , are all modelled via the maximum entropy approach. Furthermore, the general formulation allows cross-correlation between the disturbance noise, w_1 , and the observation noise, w_2 .

The object is to design a lower order dynamic controller with state $x_c \in \mathbb{R}^{N_c}$ where $N_c < N$ by choosing the controller matrices A_c , B_c and C_c so as to minimize the indicated quadratic performance criterion. Note that the possibility of cross terms ($R_{12} \neq 0$) in the performance index is accounted for in this formulation.



PERFORMANCE CRITERION

$$J(A_c, B_c, C_c) = \lim_{t \rightarrow \infty} E[x^T R_1 x + 2x^T R_{12} u + u^T R_2 u]$$

Technical Assumption: $B_i \neq 0 \Rightarrow C_i = 0$

Figure 10

MAIN THEOREM OF OP/ME: OPTIMAL COMPENSATOR GAINS

With the foregoing problem statement, the quadratically optimal gains are given by the first three expressions in Figure 11. These relationships are basically LQG in character - the major modification being brought about by the appearance of the matrices $\Gamma \in \mathbb{R}^{N_c \times N}$ and $G \in \mathbb{R}^{N_c \times N}$. A particular factorization of the optimal projection τ , i.e., $\Gamma G^T = I_{N_c}$, is represented by Γ and G so that $\tau = G^T \Gamma$ is idempotent. Note that any rank N_c projection can be factored in this way and, for given τ , any and all such factorizations yield the same closed-loop performance (see [22]).

Determination of A_c , B_c and C_c requires that we first solve the basic design equations (shown in Figure 12) for the quantities Q , P , and \hat{Q} , \hat{P} and τ . The notational conventions given on the lower half of Figure 11 serve to define these design equations precisely.

CONTROLLER GAINS (Functions of Q , P , \hat{Q} , \hat{P})

$$A_c = \Gamma(A_s - B_s R_{2s}^{-1} P_s - Q_s V_{2s}^{-1} C_s) G^T$$

$$B_c = \Gamma Q_s V_{2s}^{-1}$$

$$C_c = -R_{2s}^{-1} P_s G^T$$

NOTATION

$$\hat{Q}\hat{P} = G^T M \Gamma, \quad \Gamma G^T = I_{n_c} \quad (\Leftrightarrow \tau = G^T \Gamma = \tau^2)$$

$$AQA^T = \sum_{i=1}^p A_i Q A_i^T, \quad AQB = \sum_{i=1}^p A_i Q B_i, \text{ etc.}$$

$$A_s = A + \frac{1}{2} A^2 \quad B_s = B + \frac{1}{2} AB \quad C_s = C + \frac{1}{2} CA$$

$$R_{2s} = R_2 + B^T(P + \hat{P})B$$

$$V_{2s} = V_2 + C(Q + \hat{Q})C^T$$

$$Q_s = QC_s^T + V_{12} + A(Q + \hat{Q})C^T$$

$$P_s = B_s^T P + R_{12}^T + B^T(P + \hat{P})A$$

Figure 11

OPTIMAL PROJECTION/MAXIMUM ENTROPY DESIGN EQUATIONS

Finally, Figure 12 shows the fundamental OP/ME design equations for determination of P , Q , \hat{P} , \hat{Q} and τ . The nonnegative-definite matrices P and Q are analogous to the regulator and observer cost matrices of LQG and are determined by two modified Riccati equations. The two modified Lyapunov equations satisfied by matrices \hat{Q} and \hat{P} are analogous to the Lyapunov equations determining controllability and observability Grammians that are employed by many of the current, suboptimal, controller-order reduction schemes. Note that the optimal projection, τ , is given explicitly in terms of the group generalized inverse of the product $\hat{Q}\hat{P}$. Thus, the nonnegative-definite matrices \hat{Q} and \hat{P} largely serve to determine τ .

In contrast to LQG, all four equations are coupled both by the optimal projection and by the stochastic modification terms - indicating that the classical separation principle generally breaks down under restrictions on controller dimension and/or under the impact of parameter uncertainties.

The four equations in Figure 12 summarize a generalized LQG-type approach wherein robust controllers of low dimension follow as a direct consequence of the optimality criterion and a priori uncertainty levels. Moreover, the computational task is well-defined: solve a system of two Riccati and two Lyapunov equations coupled by the optimal projection and stochastic effects. A variety of computational procedures are presented in [1, 4, 14-15, 17, 19] and these are currently included in an automated design software package. We illustrate this automated design capability in the example problems that follow.

SOLVE FOR NONNEGATIVE-DEFINITE Q, P, \hat{Q}, \hat{P}

$$0 = A_s Q + Q A_s^T + A Q A^T + V_1 + (A - B R_{2s}^{-1} P_s) \hat{Q} (A - B R_{2s}^{-1} P_s)^T - Q_s V_{2s}^{-1} Q_s^T + \tau_1^T V_{2s}^{-1} Q_s^T \tau_1$$

$$0 = A_s^T P + P A_s + A^T P A + R_1 + (A - Q_s V_{2s}^{-1} C_s)^T \hat{P} (A - Q_s V_{2s}^{-1} C_s) - P_s^T R_{2s}^{-1} P_s + \tau_1^T P_s^T R_{2s}^{-1} P_s \tau_1$$

$$0 = (A_s - B_s R_{2s}^{-1} P_s) \hat{Q} + \hat{Q} (A_s - B_s R_{2s}^{-1} P_s)^T + Q_s V_{2s}^{-1} Q_s^T - \tau_1^T Q_s V_{2s}^{-1} Q_s^T \tau_1$$

$$0 = (A_s - Q_s V_{2s}^{-1} C_s)^T \hat{P} + \hat{P} (A_s - Q_s V_{2s}^{-1} C_s) + P_s^T R_{2s}^{-1} P_s - \tau_1^T P_s^T R_{2s}^{-1} P_s \tau_1$$

$$\text{RANK } \hat{Q} = \text{RANK } \hat{P} = \text{RANK } \hat{Q}\hat{P} = n_c$$

$$\tau = \hat{\hat{Q}}\hat{\hat{P}}(\hat{\hat{Q}}\hat{\hat{P}})^{\#} \quad \tau_1 = I_n - \tau$$

\Rightarrow GROUP GENERALIZED INVERSE

Figure 12

EXAMPLE 1: CSDL MODEL #2

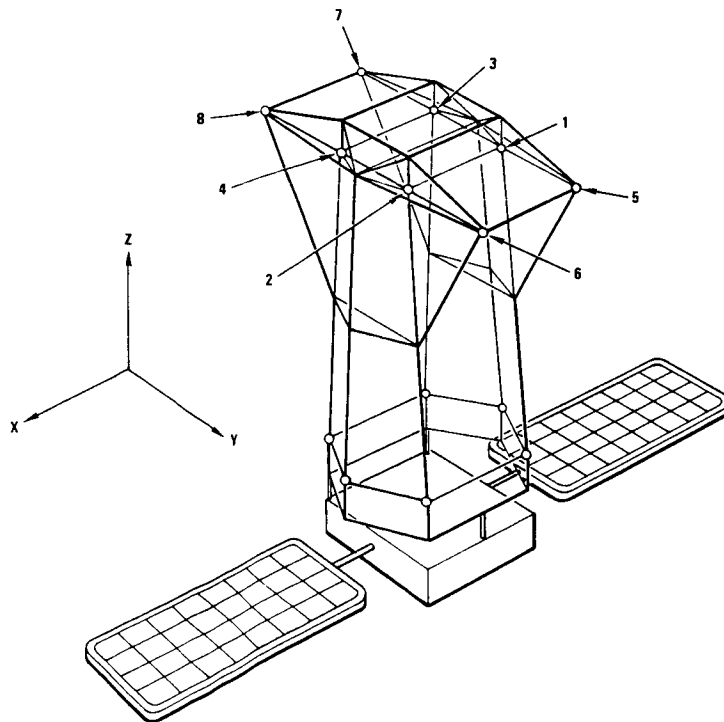
The first two examples considered here illustrate application of the optimal projection approach without inclusion of parameter uncertainty effects. The third and final example serves to illustrate the combined OP/ME design capability.

The first case was treated in [17] and is depicted in Figure 13. Specifically, it is a version of the CSDL, ACOSS Model 2 previously considered in [91]. The steady state performance index has the form

$$J = E [X^T R_1 X] + R E [U^T U]$$

where R_1 represents the state penalties on mean square line-of-sight errors and defocus and R is a positive scalar. Clearly, controller authority and bandwidth are both inversely proportional to R .

This example was used to compare both theoretically and numerically the optimal projection approach with a variety of suboptimal controller-order reduction methods. The theoretical comparison shows that all current suboptimal techniques essentially define a (suboptimal) projection characterizing the reduced-order compensator. In contrast, the optimal projection design equations define the needed projection by rigorous application of optimality principles. Moreover, all the approaches considered in [7] can be displayed in a common notation, and this graphically reveals the suboptimal design equations as special cases of or approximations to the optimal projection equations.



REFERENCE: [91]

R. E. Skelton and P. C. Hughes, "Modal Cost Analysis for Linear Matrix Second-Order Systems," J Dyn Syst Meas and Control Vol 102, September 1980, pp 151-180

Figure 13

NUMERICAL COMPARISON OF SUBOPTIMAL AND OPTIMAL PROJECTION APPROACHES

Now for the numerical comparisons. As is standard in the application of quadratic optimization, one characterizes each design for a fixed compensator order by plotting the "regulation cost" ($E[X^T R_1 X]$) as a function of the "control cost" ($E[U^T U]$). Results for these tradeoff curves are shown in Figure 14. The very bottom-most curve represents the full-order, LQG design. Since this is the best obtainable when there is no restriction on compensator order, the problem is obtaining a lower order design whose tradeoff curve is as close to the LQG results as possible.

The thin black lines in Figure 14 show the $N_C = 10, 6$, and 4 designs obtained via Component Cost Analysis [83], where N_C denotes the compensator dimension. This appears to be the most successful suboptimal method applied to the example problem considered here. Note that the 10th and 6th order compensator designs are quite good, but when compensator order is sufficiently low ($N_C = 4$) and controller bandwidth sufficiently large ($R < 5.0$), the method fails to yield stable designs. This difficulty is characteristic of all suboptimal techniques surveyed, and, in fairness, it should be noted that most other suboptimal design methods fail to give stable designs for compensator orders below 10.

In contrast, the width of the grey line in Figure 14 encompasses all the optimal projection results for compensators of orders 10, 6, and 4.

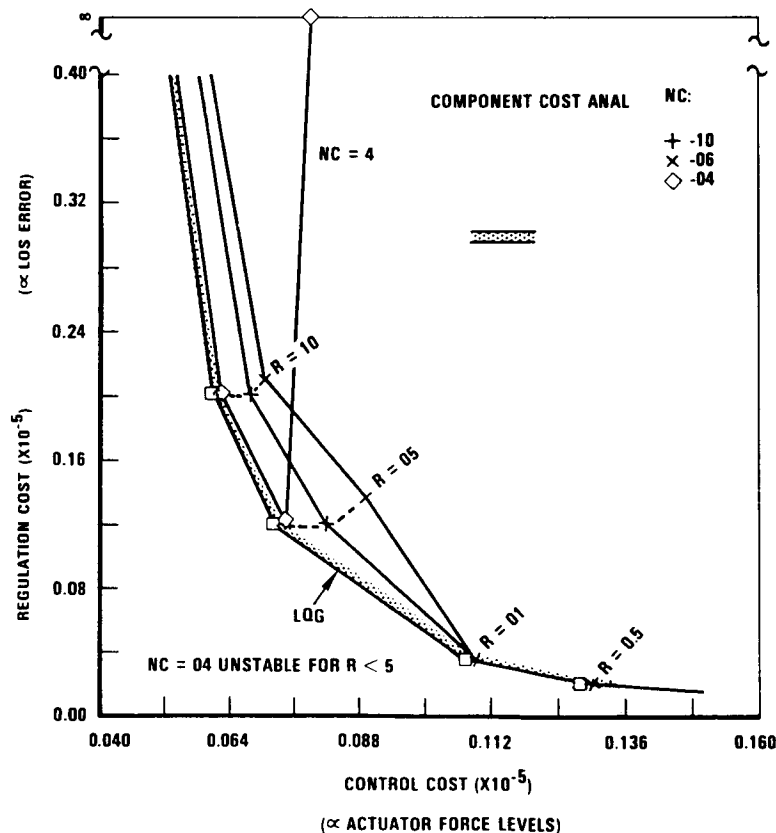


Figure 14

OPTIMAL PROJECTION RESULTS FOR PERFORMANCE/COMPLEXITY TRADEOFF

To provide a more detailed picture of the optimal projection results, Figure 15 shows the percent of total performance increase relative to the full-order, LQG designs as a function of $1/R$ (proportional to controller bandwidth and to actuator force levels) for the various compensator orders considered.

Even for the 4th order design, the optimal projection performance is only ~5 percent higher than the optimal full-order design. Furthermore, the performance index for the optimal projection designs increases monotonically with decreasing controller order - as it should. Such is not the case for suboptimal design methods.

These results reinforce our belief that the optimal projection approach is a powerful and highly reliable alternative to current reduced-order control design methods.

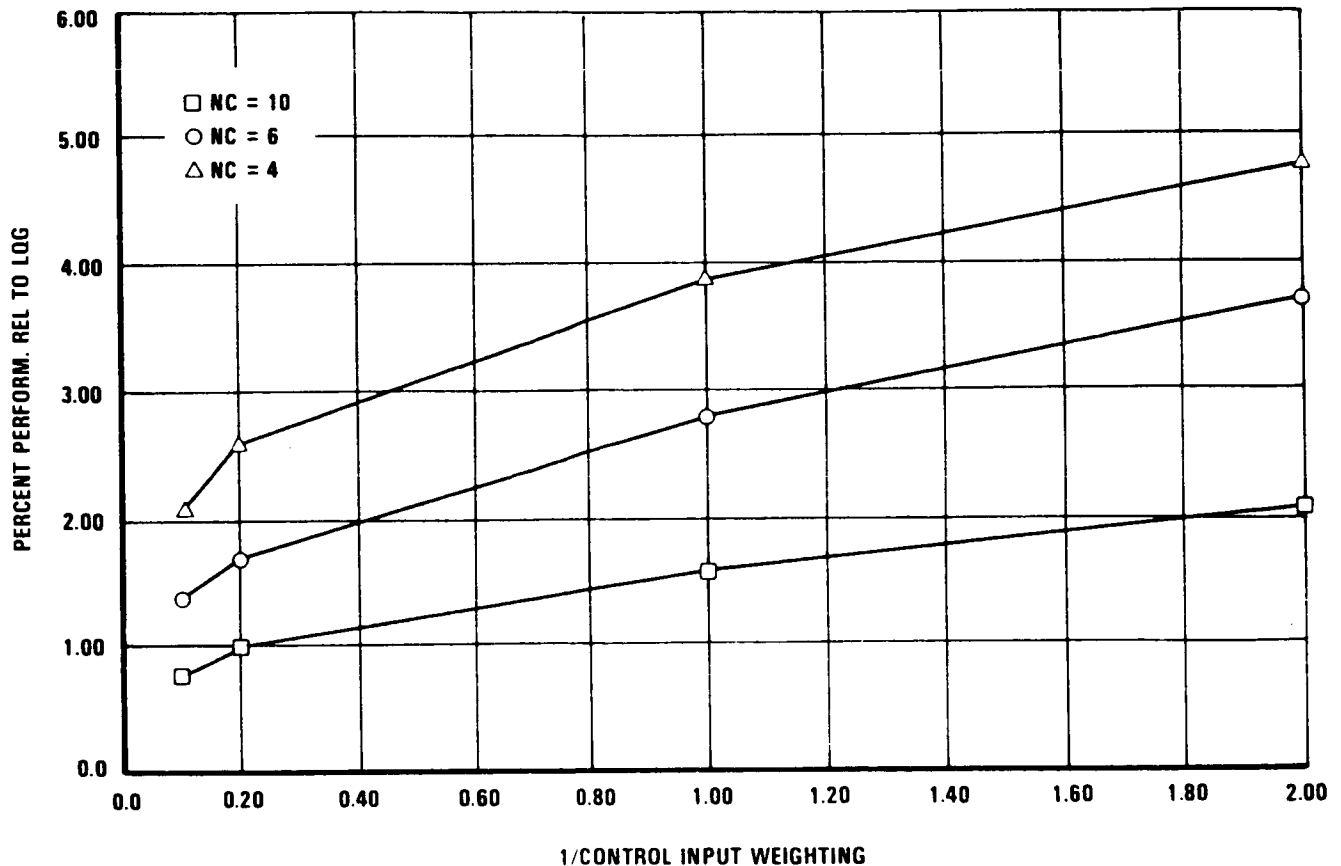


Figure 15

EXAMPLE 2: 15-M HOOP/COLUMN ANTENNA CONTROLS/DYNAMICS EXPERIMENT CONCEPT

The second example of the application of optimal projection involves significant interplay among controller design, experiment design, and control hardware selection.

To further the technology development goals of the planned Large Space Antenna Flight Experiment, Harris GASD has undertaken a preliminary study for design of a ground-based controls and dynamics experiment involving the 15-M Hoop/Column Antenna. This structure is a deployable mesh reflector design for space communications applications.

In designing the experimental apparatus, it was our goal to establish performance requirements, disturbance spectra, etc., to emulate (not simulate a flight test) the generic pathologies of large space systems. Care was also taken in selecting control hardware and software in such a way as to provide a good test-bed for a variety of system identification and control design approaches.

The basic experimental configuration motivated by the above considerations is depicted in Figure 16. As shown, the entire spacecraft is suspended by a cable secured to the ceiling of a radome. The point of attachment to the structure is inside the primary column segment approximately 1.5 inches above the center of mass. The resulting gravity moment arm provides some slight restoring stiffness and prevents the cable from resting against the column. Absence of an RF feed (replaced by equivalent weights) permits the suspending cable to run clear through the aperture of the upper column segment, thereby permitting approximately 5° of rotational motion along both horizontal axes.

Steady-state random disturbances are to be supplied by two-axis torquers located within the spacecraft bus. The selected location provides significant disturbability to the first hundred modes and a high degree of disturbance to ~50 modes.

15-METER H/C MODEL CABLE SUSPENDED CONFIGURATION FOR GROUND TESTING

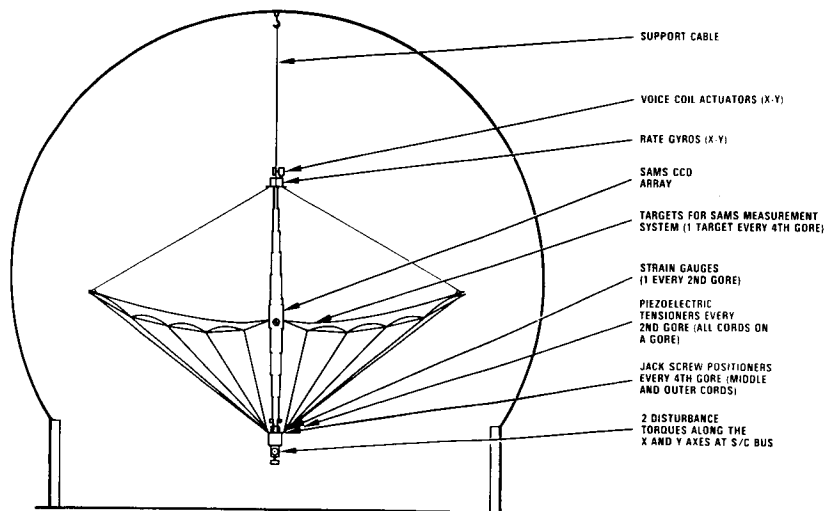
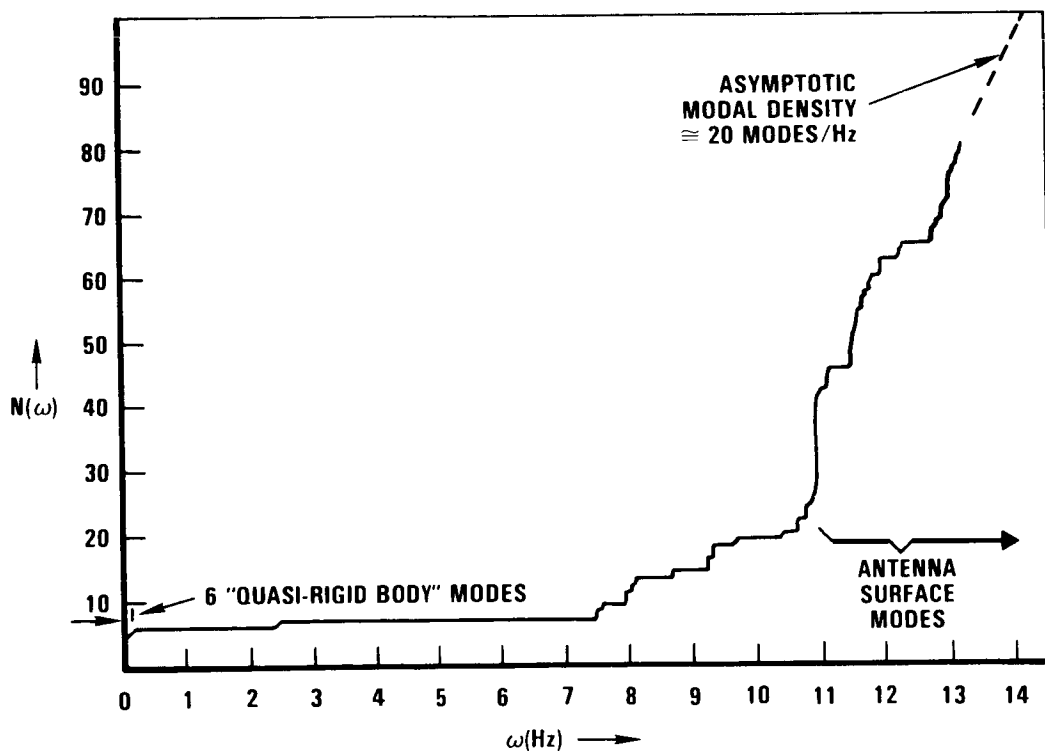


Figure 16

DISTRIBUTION OF MODAL FREQUENCIES FOR 15M CONTROLS/DYNAMICS EXPERIMENT CONCEPT

Detailed finite element analyses of this cable-suspended configuration have been carried out, and the overall distribution of modal frequencies can be summarized as in Figure 17. The figure shows the "mode-count" versus frequency; i.e., $N(\omega)$ denotes the number of modes below a given frequency, ω . As indicated, there is a collection of "quasi-rigid-body" nodes at low frequencies. Each of these modes involves a compound pendulum motion on the cable with the spacecraft undergoing essentially rigid-body rotations and translations. The quasi-rigid-body modes provide a rather accurate simulation of rigid body degrees of freedom. At ~ 7.5 Hz and above, there emerge the overall beam bending or "spacecraft" modes involving bending of the supporting hoop and central column. Finally, the rapid increase in mode count above ~ 11 Hz is accounted for by the very closely spaced "antenna surface" modes - involving motion primarily of the mesh surface and its underlying tensioning and control cords.

$N(\omega) \triangleq$ NUMBER OF MODAL FREQUENCIES BELOW ω



15-M MODEL GROUND TEST CONFIGURATION MODE-COUNT VERSUS FREQUENCY

Figure 17

15-M EXPERIMENT - INSTRUMENTATION CONCEPT AND DESIGN RESULTS

Because there is a wide dispersion of disturbability for the selected disturbance source, it is possible to deliberately shape the disturbance spectrum to provide significant excitation of a desired number of modes. The selected spectrum is broad band with a half-power band limit of 15 Hz. As is evident from Figure 17, the 15 Hz bandwidth easily covers more than 100 modes.

Of course, significant disturbance on a large number of modes does not alone suffice to create a challenging control problem - selection and scaling of performance criteria are also necessary tasks in the experiment design. Refs. [92, 93] give details on the selected quadratic performance index. Basically, the state penalty consists of three main terms which impose performance penalties on (1) pointing errors, (2) misalignment and defocus errors, and (3) antenna surface shape errors.

With the control objectives thus defined, the control design and actuator/sensor selection methodologies were exercised iteratively to obtain a set of applicable, low-cost devices. The resulting instrumentation plan is depicted in Figure 18 a and detailed in [93].

Design results including dynamics models for the full complement of control hardware devices indicated in Figure 18 b are reported in [93]. For simplicity, we consider results on a subproblem involving only elastic mode vibration control using four jackscrew positioner devices and four strain gauges mounted on the control cords.

Despite a large number of modes included in the design model, optimal projection designs were successfully obtained and the effect of decreasing the control input penalty (progressively increasing the control authority) on closed-loop system poles is indicated in Figure 18 b. It is seen that while high order modes remain stable, significant increases in damping can be achieved for lower order modes within the limitations (force/bandwidth) of the actuators and sensors.

OVERALL EXPERIMENT HARDWARE CONCEPT

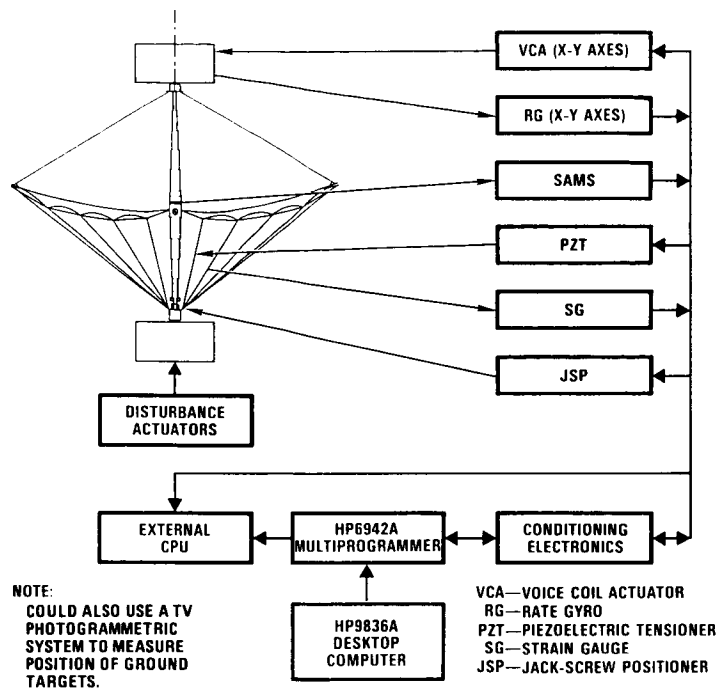


Figure 18 a

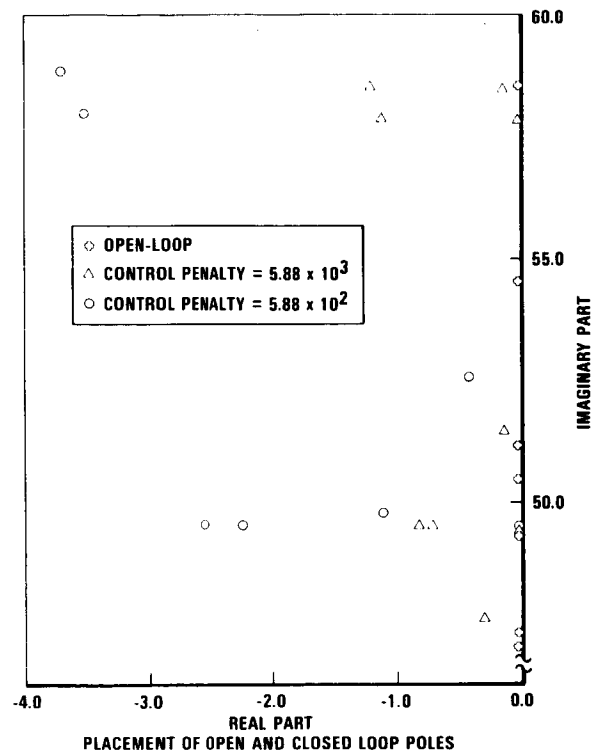


Figure 18 b

15-M EXPERIMENT: PERFORMANCE/COMPLEXITY TRADEOFF RESULTS

For the problem considered above, Figure 19 summarizes the tradeoffs of performance versus controller complexity (compensator dimension) and control authority (control input weighting in the performance index). Generally, it is seen that compensators of dimension > 10 yield negligible improvement in performance. This conclusion holds for the general problem including all hardware devices and rigid body modes. Thus, memory and throughput requirements for the processor needed to implement the control algorithm were sized on the assumption that $N_c \leq 10$. These estimates were then used to arrive at the processor selection indicated in Figure 18.a. Specifically, the control algorithm would be implemented on the HP 9836A Desktop Computer. This is a Motorola MC68000 microprocessor-based (16-bit) machine. Also, the HP-6942A Multiprogrammer can be utilized to perform all a/d and d/a conversions as well as data handling. An external CPU is included to assist in data handling and route data to off-line storage. After completion of a given experimental sequence, stored data can be analyzed, parameter identification tests can be performed and results can be correlated with analytical predictions.

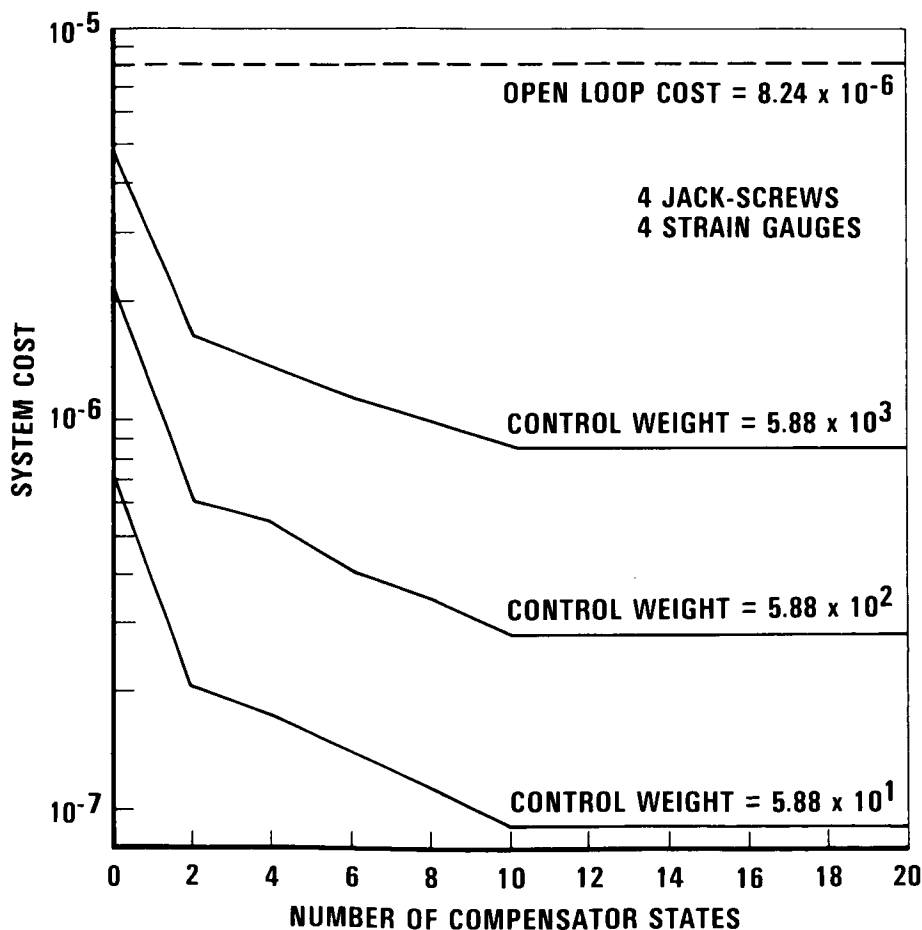


Figure 19

EXAMPLE 3: SPACECRAFT CONTROL LABORATORY EXPERIMENT (SCOLE)

Our third and last example is used primarily to illustrate application of the maximum entropy design-for-uncertainty approach. Harris GASD has just completed a NASA LaRC supported study on the Spacecraft Control Laboratory Experiment (SCOLE) configuration shown in Figure 20. This is the subject of the NASA/IEEE Design Challenge described in [94]. Since the study is specifically aimed at exploring the maximum entropy approach, its scope is restricted in other areas. Specifically, we consider the steady state pointing problem using linear, continuous-time models of all subsystems.

A high order finite element model was constructed for SCOLE, treating the Shuttle and reflectors as rigid bodies and the connecting mast as a classical beam with torsional stiffness. This model includes the Shuttle products-of-inertia and the offset between reflector center-of-mass and its attachment point on the mast. The quadratic performance penalty on the system state is simply the total mean square line of sight error (as defined in [94]). Full details of our model and design results are given in [95].

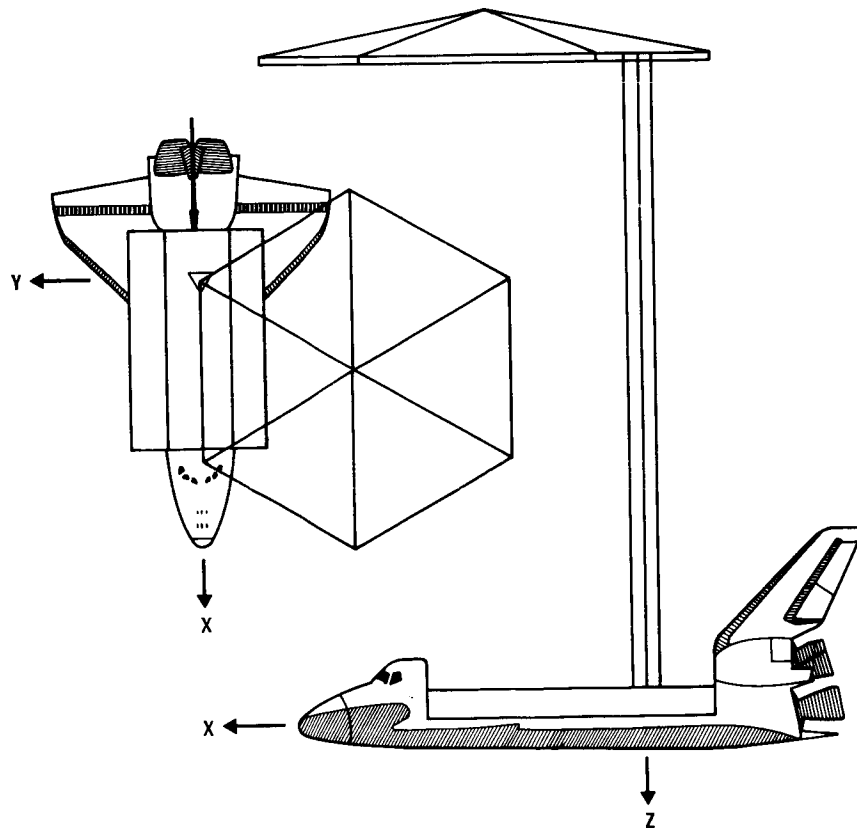


Figure 20

COMPARISON OF CLOSED-LOOP POLE SENSITIVITY FOR LQG AND MAXIMUM ENTROPY DESIGNS

As part of the SCOLE study, we considered a system model including the first eight modes and (1) performed LQG studies to select the control authority and establish a baseline and (2) designed full-order (16 state) compensators with a maximum entropy model of modal frequency uncertainties. The maximum entropy model assumed that all elastic mode frequencies were subjected to independent variations (due to modelling error) of $+\sigma$ to $-\sigma$ relative to their nominal values. Thus the positive number σ denotes the overall fractional uncertainty.

Although robust stability is obtained under these independent and simultaneous variations, the robustness properties of specific designs are simply illustrated here by looking at the variation of performance and closed-loop poles when all modal frequencies are varied by the same fractional change from the nominal values. In other words, we interconnect a given controller design (be it LQG or maximum entropy) with a perturbed plant model wherein all modal frequencies are changed by δx (nominal values) and evaluate the closed-loop performance and pole locations. This is repeated for a range of values of δ .

Figure 21 a shows how the pole locations for an LQG design wander under a $\pm 5\%$ variation of the modal frequencies. It is seen that two of the pole pairs are particularly sensitive and are nearly driven unstable by only this $\pm 5\%$ variation. This happens because the associated structural modes contribute little to performance and the LQG design attempts a "cheap control" (small regulator and observer gains) by placing compensator poles very close to the open-loop plant poles. For nominal values, this scheme achieves significant shifts of open-loop poles with very small gains, but it is highly sensitive to off-nominal perturbations.

Figure 21 b shows closed-loop poles for the same conditions except that a maximum entropy compensator design with $\sigma = 0.1$ (10% variation modelled) was utilized. In contrast with Figure 21 a, the maximum entropy design makes the compensator poles "stand-off" deeper in the left half plane. (This is a direct consequence of the Stratonovich correction.) Consequently, the strong and sensitive interactions noted above are entirely eliminated. The poles associated with higher-order structural modes are seen to vary only along the imaginary axis and are not destabilized.

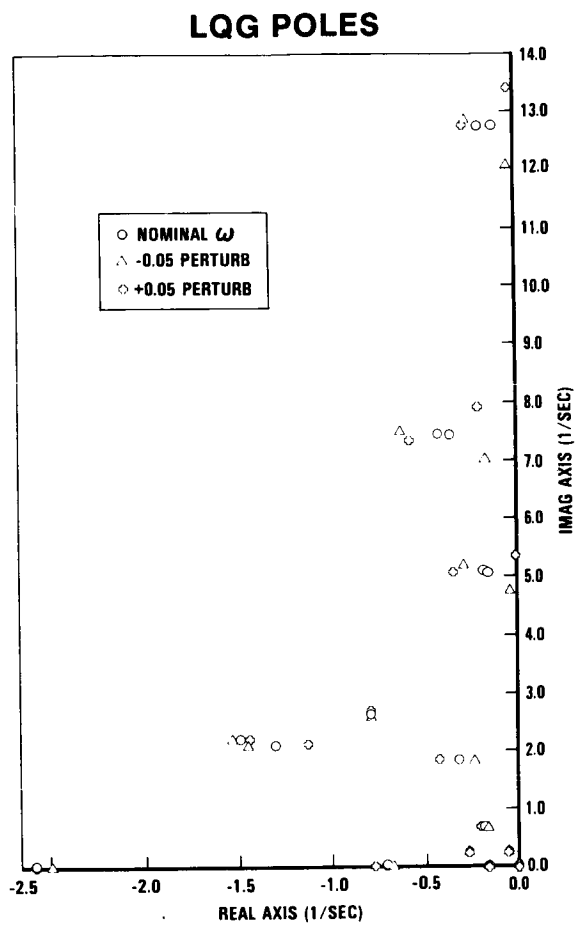


Figure 21 a

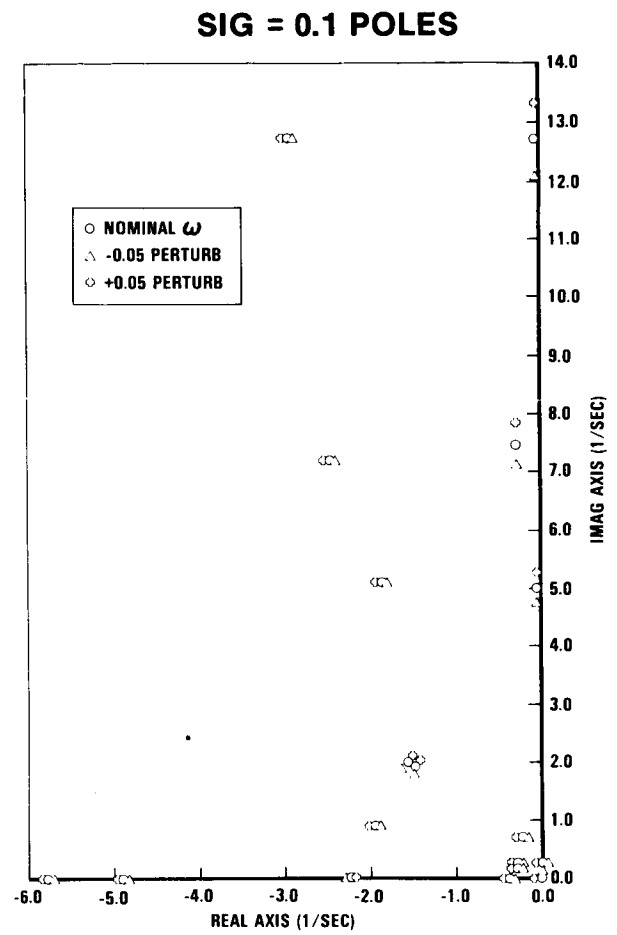


Figure 21 b

VARIATION OF PERFORMANCE WITH SYSTEM PARAMETER DEVIATIONS:
DETERMINISTIC MODELLING VERSUS MAXIMUM ENTROPY DESIGN

Figure 22 illustrates how the total performance index for given controller designs varies as the structural mode frequencies are perturbed relative to their nominal values. The LQG design (which is simply a maximum entropy design for $\sigma = 0$) becomes unstable for $> 7\%$ and $< -14\%$ variations. In contrast and even with a modest 10% level of modelled uncertainty, the maximum entropy designs completely eliminate the sensitivity. Note that within the parameter range for which LQG is stable, the $\sigma = 0.1$ maximum entropy design experiences only a ~12-15% degradation. Of course, over the regions for which LQG is unstable, the maximum entropy designs are qualitatively superior.

These results serve to illustrate a general fact: By incorporating parameter uncertainty as an intrinsic facet of the basic design model, the maximum entropy formulation is able to secure high levels of robustness with little degradation of nominal performance.

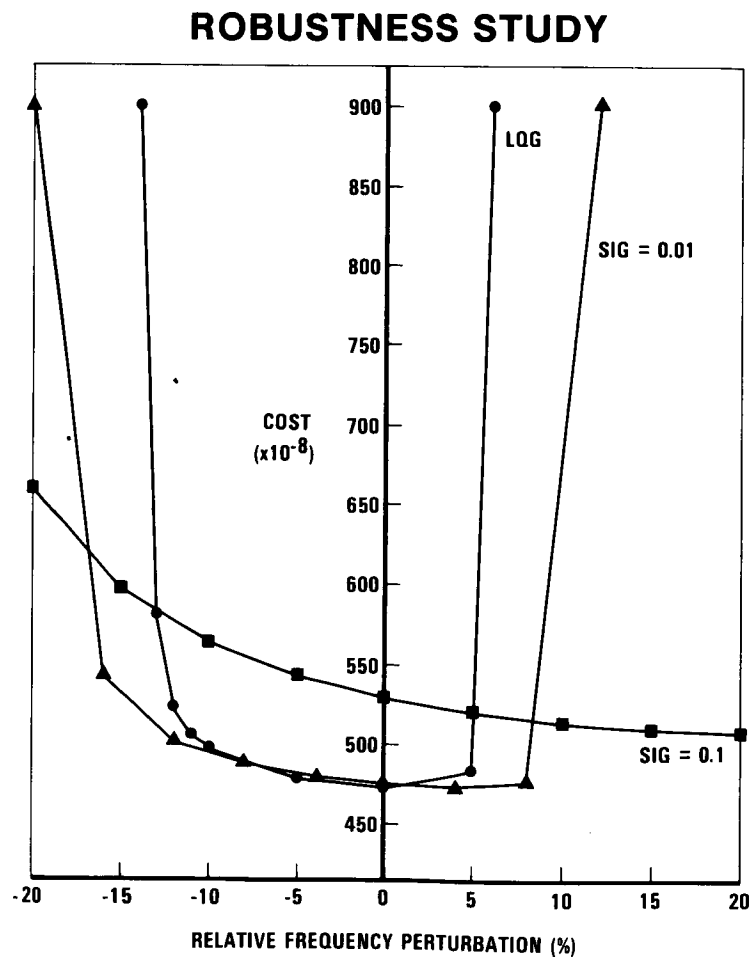


Figure 22

COMBINED OP/ME DESIGN: PERFORMANCE/COMPLEXITY TRADEOFF

Finally, the combined OP/ME design capability was exercised, taking the 16-state maximum entropy compensator design with $\sigma = 0.10$ frequency uncertainty level as the starting point. Reduced order compensator designs were constructed for compensators of order 14, 12, 10, 8, 6 and 5. Figure 23 shows the tradeoff between performance (total, closed-loop performance index evaluated for nominal values of modal frequencies) and controller dimension. The Figure clearly shows that performance degradation for compensator orders above 6 is negligible. The 6th order controller sacrifices only 3% of the performance of the full-order (16 state) controller. This would seem to be acceptable in view of the better than sixfold decrease in implementation costs (e.g., flops required in matrix multiplication) which results from order reduction.

In conclusion, these results, together with much additional material included in [95], demonstrate automated solution of the full OP/ME design equations (shown in Figure 12) and illustrate the performance and implementation benefits to be expected under this unified approach.

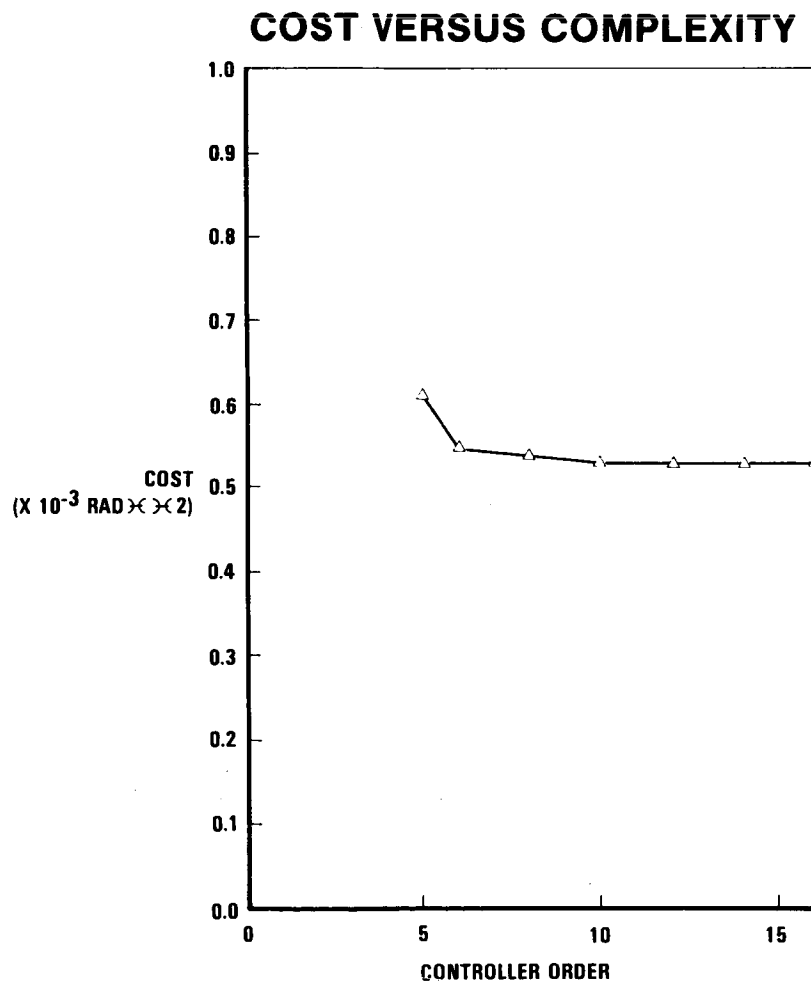


Figure 23

References

1. D. C. Hyland, "Optimal Regulation of Structural Systems With Uncertain Parameters," MIT, Lincoln Laboratory, TR-551, 2 February 1981, DDC# AD-A099111/7.
2. D. C. Hyland, "Active Control of Large Flexible Spacecraft: A New Design Approach Based on Minimum Information Modelling of Parameter Uncertainties," VPI&SU/AIAA Symposium, Blacksburg, VA, June 1981.
3. D. C. Hyland, "Optimal Regulator Design Using Minimum Information Modelling of Parameter Uncertainties: Ramifications of the New Design Approach," VPI&SU/AIAA Symposium, Blacksburg, VA, June 1981.
4. D. C. Hyland and A. N. Madiwale, "Minimum Information Approach to Regulator Design: Numerical Methods and Illustrative Results," VPI&SU/AIAA Symposium, Blacksburg, VA, June 1981.
5. D. C. Hyland and A. N. Madiwale, "A Stochastic Design Approach for Full-Order Compensation of Structural Systems with Uncertain Parameters," AIAA Guidance and Control Conference, Albuquerque, NM, August 1981.
6. D. C. Hyland, "Optimality Conditions for Fixed-Order Dynamic Compensation of Flexible Spacecraft with Uncertain Parameters," AIAA 20th Aerospace Sciences Meeting, Orlando, FL, January 1982.
7. D. C. Hyland, "Structural Modeling and Control Design Under Incomplete Parameter Information: The Maximum Entropy Approach," Modelling, Analysis and Optimization Issues for Large Space Structures, NASA CP-2258, 1983, pp.73-96.
8. D. C. Hyland, "Maximum Entropy Stochastic Approach to Control Design for Uncertain Structural Systems," American Control Conference, Arlington, VA, June 1982.
9. D. C. Hyland, "Minimum Information Stochastic Modelling of Linear Systems with a Class of Parameter Uncertainties," American Control Conference, Arlington, VA, June 1982.
10. D. C. Hyland and A. N. Madiwale, "Fixed-Order Dynamic Compensation Through Optimal Projection," Proceedings of the Workshop on Applications of Distributed System Theory to the Control of Large Space Structures, JPL, Pasadena, CA, July 1982.
11. D. C. Hyland, "Minimum Information Modelling of Structural Systems with Uncertain Parameters," Proceedings of the Workshop on Applications of Distributed System Theory to the Control of Large Space Structures, JPL, Pasadena, CA, July 1982.
12. D. C. Hyland, "Mean-Square Optimal Fixed-Order Compensation - Beyond Spillover Suppression," AIAA Astrodynamics Conference, San Diego, CA, August 1982.
13. D. C. Hyland, "Robust Spacecraft Control Design in the Presence of Sensor/Actuator Placement Errors," AIAA Astrodynamics Conference, San Diego, CA, August 1982.

14. D. C. Hyland, "The Optimal Projection Approach to Fixed-Order Compensation: Numerical Methods and Illustrative Results," AIAA 21st Aerospace Sciences Meeting, Reno, NV, January 1983.
15. D. C. Hyland, "Mean-Square Optimal, Full-Order Compensation of Structural Systems with Uncertain Parameters," MIT, Lincoln Laboratory TR-626, 1 June 1983.
16. D. C. Hyland and D. S. Bernstein, "The Optimal Projection Equations for Fixed-Order Dynamic Compensation," IEEE Trans. Autom. Contr., Vol. AC-29, pp. 1034-1037, 1984.
17. D. C. Hyland, "Comparison of Various Controller-Reduction Methods: Suboptimal Versus Optimal Projection," Proc. AIAA Dynamics Specialists Conference, Palm Springs, CA, May 1984.
18. D. S. Bernstein and D. C. Hyland, "The Optimal Projection Equations for Fixed-Order Dynamic Compensation of Distributed Parameter Systems," Proc. AIAA Dynamics Specialists Conference, Palm Springs, CA, May 1984.
19. D. S. Bernstein and D. C. Hyland, "Numerical Solution of the Optimal Model Reduction Equations," AIAA Guidance and Control Conference, Seattle, WA, August 1984.
20. D. C. Hyland and D. S. Bernstein, "The Optimal Projection Approach to Model Reduction and the Relationship Between the Methods of Wilson and Moore," 23rd IEEE Conference on Decision and Control, Las Vegas, NV, December 1984.
21. D. S. Bernstein and D. C. Hyland, "The Optimal Projection Approach to Designing Optimal Finite-Dimensional Controllers for Distributed-Parameter Systems" 23rd IEEE Conference on Decision and Control, Las Vegas, NV, December 1984.
22. D. C. Hyland and D. S. Bernstein, "The Optimal Projection Equations for Fixed-Order Dynamic Compensation," IEEE Trans. Autom. Contr., Vol. AC-29, No. 11, pp. 1034-1037, 1984.
23. D. S. Bernstein and D. C. Hyland, "The Optimal Projection Equations for Finite-Dimensional Fixed-Order Dynamic Compensation of Infinite-Dimensional Systems," SIAM J. Contr. Optim., Vol. 24, pp. 122-151, 1986.
24. D. C. Hyland and D. S. Bernstein, "The Optimal Projection Equations for Model Reduction and the Relationships Among the Methods of Wilson, Skelton and Moore," IEEE Trans. Autom. Contr., Vol. AC-30, 1985.
25. D. C. Hyland and D. S. Bernstein, "The Optimal Projection Equations for Reduced-Order State Estimation," IEEE Trans. Autom. Contr., Vol. AC-30, pp. 583-585, 1985.
26. E. T. Jaynes, "New Engineering Applications of Information Theory," Proceedings of the First Symposium on Engineering Applications of Random Function Theory and Probability, J. L. Bogdanoff and F. Kozin, pp. 163-203, Wiley, New York, 1963.

27. E. T. Jaynes, "Prior Probabilities," IEEE Trans. Sys. Sci. Cybern., Vol. SSC-4, pp. 227-241, 1968.
28. E. T. Jaynes, "Where Do We Stand on Maximum Entropy," The Maximum Entropy Formalism, D. Levine and M. Tribus, eds., The MIT Press, pp. 15-118, Cambridge, MA, 1979.
29. R. D. Rosenkrantz, ed., "E. T. Jaynes: Papers on Probability, Statistics and Statistical Physics," Reidel, Boston, 1983.
30. K. Ito, On Stochastic Differential Equations, Amer. Math. Soc., Providence, RI, 1951.
31. E. Wong and M. Zakai, "On the Relation Between Ordinary and Stochastic Differential Equations," Int. J. Engrg. Sci., Vol. 3, pp. 213-229, 1965.
32. R. L. Stratonovich, "A New Representation for Stochastic Integrals," SIAM J. Contr., Vol. 4, pp. 362-371, 1966.
33. R. L. Stratonovich, Conditional Markov Process and Their Application to the Theory of Optimal Control, Elsevier, NY, 1968.
34. A. H. Jazwinski, Stochastic Processes and Filtering Theory, Academic Press, New York, 1970.
35. E. Wong, Stochastic Processes in Information and Dynamical Systems, McGraw-Hill, New York, 1971.
36. E. J. McShane, Stochastic Calculus and Stochastic Models, Academic Press, Press, New York, 1974.
37. L. Arnold, Stochastic Differential Equations: Theory and Applications, Wiley, New York, 1974.
38. W. H. Fleming and R. W. Rishel, Deterministic and Stochastic Optimal Control, Springer-Verlag, New York, 1975.
39. H. J. Sussmann, "On the Gap Between Deterministic and Stochastic Ordinary Differential Equations," The Annals of Probability, Vol. 6, pp. 19-41, 1978.
40. W. M. Wonham, "Optimal Stationary Control of Linear Systems with State-Dependent Noise," SIAM J Contr., Vol. 5, pp. 486-500, 1967.
41. M. Metivier and J. Pellaumail, Stochastic Integration, Academic Press, New York, 1980.
42. W. M. Wonham, "On a Matrix Riccati Equation of Stochastic Control," SIAM J. Contr., Vol. 6, pp. 681-697, 1968.
43. W. M. Wonham, "Random Differential Equations in Control Theory," in Probabilistic Analysis in Applied Mathematics, A. T. Bharucha-Reid, ed., Vol. 2, pp. 131-212, Academic Press, New York, 1970.
44. D. Kleinman, "Optimal Stationary Control of Linear Systems with Control-Dependent Noise," IEEE Trans. Autom. Contr., Vol. AC-14, pp. 673-677, 1969.

45. P. J. McLane, "Optimal Linear Filtering for Linear Systems with State-Dependent Noise," Int. J. Contr., Vol. 10, pp. 41-51, 1969.
46. P. McLane, "Optimal Stochastic Control of Linear Systems with State- and Control-Dependent Disturbances," IEEE Trans. Autom. Contr., Vol. AC-16, pp. 793-798, 1971.
47. D. Kleinman, "Numerical Solution of the State Dependent Noise Problem," IEEE Trans. Autom. Contr., Vol. AC-21, pp. 419-420, 1976.
48. U. Haussmann, "Optimal Stationary Control with State and Control Dependent Noise," SIAM J. Contr., Vol. 9, pp. 184-198, 1971.
49. J. Bismut, "Linear-Quadratic Optimal Stochastic Control with Random Coefficients," SIAM J. Contr., Vol. 14, pp. 419-444, 1976.
50. A. Ichikawa, "Optimal Control of a Linear Stochastic Evolution Equation with State and Control Dependent Noise," Proc. IMA Conference on Recent Theoretical Development in Control, Leicester, England, Academic Press, New York, 1976.
51. A. Ichikawa, "Dynamic Programming Approach to Stochastic Evolution Equations," SIAM J. Contr. Optim., Vol 17, pp. 152-174, 1979.
52. N. U. Ahmed, "Stochastic Control on Hilbert Space for Linear Evolution Equations with Random Operator-Valued Coefficients," SIAM J. Contr. Optim., Vol. 19, pp. 401-430.
53. C. W. Merriam III, Automated Design of Control Systems, Gordon and Breach, New York, 1974.
54. M. Aoki, "Control of Linear Discrete-Time Stochastic Dynamic Systems with Multiplicative Disturbances," IEEE Trans. Autom. Contr., Vol. AC-20, pp. 388-392, 1975.
55. D. E. Gustafson and J. L. Speyer, "Design of Linear Regulators for Nonlinear Systems," J. Spacecraft and Rockets, Vol. 12, pp. 351-358, 1975.
56. D. E. Gustafson and J. L. Speyer, "Linear Minimum Variance Filters Applied to Carrier Tracking," IEEE Trans. Autom. Contr., Vol. AC-21, pp. 65-73, 1976.
57. G. N. Milshtein, "Design of Stabilizing Controller With Incomplete State Data for Linear Stochastic System with Multiplicative Noise," Autom. and Remote Contr., Vol. 43, pp. 653-659, 1982.
58. M. Athans, R. T. Ku and S. B. Gershwin, "The Uncertainty Threshold Principle: Some Fundamental Limitations of Optimal Decision Making Under Dynamic Uncertainty," IEEE Trans. Autom. Contr., Vol. AC-22, pp. 491-495, 1977.
59. R. J. Ku and M. Athans, "Further Results on the Uncertainty Threshold Principle," IEEE Trans. Autom. Contr., Vol. AC-22, pp. 866-868, 1977.
60. T. L. Johnson and M. Athans, "On the Design of Optimal Constrained Dynamic Compensators for Linear Constant Systems," IEEE Trans. Autom. Contr., Vol. AC-15, pp. 658-660, 1970.

61. W. S. Levine, T. L. Johnson and M. Athans, "Optimal Limited State Variable Feedback Controllers for Linear Systems," IEEE Trans. Autom. Contr., Vol. AC-16, pp. 785-793, 1971.
62. K. Kwakernaak and R. Sivan, Linear Optimal Control Systems, Wiley-Interscience, New York, 1972.
63. D. B. Rom and P. E. Sarachik, "The Design of Optimal Compensators for Linear Constant Systems with Inaccessible States," IEEE Trans. Autom. Contr., Vol. AC-18, pp. 509-512, 1973.
64. M. Sidar and B.-Z. Kurtaran, "Optimal Low-Order Controllers for Linear Stochastic Systems," Int. J. Contr., Vol. 22, pp. 377-387, 1975.
65. J. M. Mendel and J. Feather, "On the Design of Optimal Time-Invariant Compensators for Linear Stochastic Time-Invariant Systems," IEEE Trans. Autom. Contr., Vol. AC-20, pp. 653-657, 1975.
66. S. Basuthakur and C. H. Knapp, "Optimal Constant Controllers for Stochastic Linear Systems," IEEE Trans. Autom. Contr., AC-20, pp. 664-666, 1975.
67. R. B. Asher and J. C. Durrett, "Linear Discrete Stochastic Control with a Reduced-Order Dynamic Compensator," IEEE Trans. Autom. Contr., Vol. AC-21, pp. 626-627, 1976.
68. W. J. Naeije and O. H. Bosgra, "The Design of Dynamic Compensators for Linear Multivariable Systems," 1977 IFAC, Fredricton, NB, Canada, pp. 205-212.
69. H. R. Sirisena and S. S. Choi, "Design of Optimal Constrained Dynamic Compensators for Non-Stationary Linear Stochastic Systems," Int. J. Contr., Vol. 25, pp. 513-524, 1977.
70. P. J. Blanvillain and T. L. Johnson, "Invariants of Optimal Minimal-Order Observer Based Compensators," IEEE Trans. Autom. Contr., Vol. AC-23, pp. 473-474, 1978.
71. C. J. Wenk and C. H. Knapp, "Parameter Optimization in Linear Systems with Arbitrarily Constrained Controller Structure," IEEE Trans. Autom. Contr., Vol. AC-25, pp. 496-500, 1980.
72. J. O'Reilly, "Optimal Low-Order Feedback Controllers for Linear Discrete-Time Systems," in Control and Dynamic Systems, Vol. 16, edited C. T. Leondes, ed., Academic Press, 1980.
73. D. P. Looze and N. R. Sandell, Jr., "Gradient Calculations for Linear Quadratic Fixed Control Structure Problems," IEEE Trans. Autom. Contr., Vol. AC-25, pp. 285-8, 1980.
74. M. Aoki, "Control of Large-Scale Dynamic Systems by Aggregation," IEEE Trans. Auto. Contr., Vol. AC-13, pp. 246-253, 1968.

75. R. E. Skelton, "Cost Decomposition of Linear Systems with Application to Model Reduction," Int. J. Contr., Vol. 32, pp. 1031-1055, 1980.
76. B. C. Moore, "Principal Component Analysis in Linear Systems: Controllability, Observability, and Model Reduction," IEEE Trans. Autom. Contr., Vol. AC-26, pp. 17-32, 1981.
77. L. Pernebo and L. M. Silverman, "Model Reduction via Balanced State Space Representations," IEEE Trans. Autom. Contr., Vol. AC-27, pp. 382-387, 1982.
78. K. V. Fernando and H. Nicholson, "On the Structure of Balanced and Other Principal Representations of SISO Systems," IEEE Trans. Autom. Contr., Vol. AC-28, pp. 228-231, 1983.
79. S. Shokoohi, L. M. Silverman, and P. M. Van Dooren, "Linear Time-Variable Systems: Balancing and Model Reduction," IEEE Trans. Autom. Contr., Vol. AC-28, pp. 810-822, 1983.
80. E. I. Verriest and T. Kailath, "On Generalized Balanced Realization," IEEE Trans. Autom. Contr., Vol. AC-28, pp. 833-844, 1983.
81. E. A. Jonckheere and L. M. Silverman, "A New Set of Invariants for Linear Systems - Application to Reduced-Order Compensator Design," IEEE Trans. Autom. Contr., Vol. AC-28, pp. 953-964, 1983.
82. R. E. Skelton and A. Yousuff, "Component Cost Analysis of Large Scale Systems," Int. J. Contr., Vol. 37, pp. 285-304, 1983.
83. A. Yousuff and R. E. Skelton, "Controller Reduction by Component Cost Analysis," IEEE Trans. Autom. Contr., Vol. AC-29, pp. 520-530, 1984.
84. J. S. Gibson, "An Analysis of Optimal Modal Regulation: Convergence and Stability," SIAM J. Contr. Optim., 19(1981), pp. 686-707.
85. J. S. Gibson, "Linear-Quadratic Optimal Control of Hereditary Differential Systems: Infinite Dimensional Riccati Equations and Numerical Approximations," SIAM J. Contr. Optim., 21(1983), pp. 95-139.
86. H. T. Banks and K. Kunisch, "The Linear Regulator Problem for Parabolic Systems," SIAM J. Contr. Optim., 22(1984), pp. 684-698.
87. H. T. Banks, K. Ito and I. G. Rosen, "A Spline Based Technique for Computing Riccati Operators and Feedback Controls in Regulator Problems for Delay Equations," ICASE Report 82-31, Institute for Computer Applications in Science and Engineering, Hampton, VA, 1982; SIAM J. Sci. Stat. Comput., 5(1984).
88. T. L. Johnson, "Optimization of Low Order Compensators for Infinite Dimensional Systems," Proc. of 9th IFIP Symp. on Optimization Techniques, Warsaw, Poland, September 1979.
89. R. K. Pearson, "Optimal Fixed-Form Compensators for Large Space Structures," in ACOSS SIX (Active Control of Space Structures), RADC-TR-81-289, Final Technical Report, Rome Air Development Center, Griffiss AFB, New York, 1981.

90. R. K. Pearson, "Optimal Velocity Feedback Control of Flexible Structures, Ph.D. Dis., MIT. Dept. Elec. Eng. Comp. Sci., 1982.
91. R. E. Skelton and P. C. Hughes, "Modal Cost Analysis for Linear Matrix Second-Order Systems," J. Dyn. Syst. Meas. and Contr., Vol. 102, pp. 151-180, September 1980.
92. F. M. Ham, J. Shipley and D. C. Hyland, "Design of a Large Space Structure Vibration Control Experiment," 2nd IMAC, Orlando, FL, February 1984.
93. F. M. Ham and D. C. Hyland, "Vibration Control Experiment Design for the 15-M Hoop/Column Antenna," JPL Workshop on Identification and Control of Flexible Space Structures, San Diego, CA, June 1984.
94. L. W. Taylor and A. V. Balakrishnan, "A Mathematical Problem and a Spacecraft Control Laboratory Experiment (SCOLE) Used to Evaluate Control Laws for Flexible Spacecraft ... NASA/IEEE Design Challenge," NASA/IEEE Report, June, 1984.
95. D. C. Hyland and L. Davis, "Application of the Maximum Entropy Design Approach to the Spacecraft Control Laboratory Experiment (SCOLE)," presented at SCOLE Workshop, December 6-7, 1984, NASA Langley Research Center.